Journal of Neurology (2019) 266:2786–2795
https://doi.org/10.1007/s00415-019-09490-y

ORIGINAL COMMUNICATION

Optimizing 3D FLAIR to detect MS lesions: pushing past factory settings for precise results

Augustin Lecler[1] · C. Bouzad[1,2] · R. Deschamps[3] · F. Maizeroi[1] · J. C. Sadik[1] · A. Gueguen[3] · O. Gout[3] · H. Picard[4] · J. Savatovsky[1]

Received: 13 May 2019 / Revised: 15 July 2019 / Accepted: 28 July 2019 / Published online: 1 August 2019

Abstract

Background To assess the diagnostic value of three 3D FLAIR sequences with differing repetition-times (TR) at 3-Tesla when detecting multiple sclerosis (MS) lesions.

Methods In this prospective study, approved by the institutional review board, 27 patients with confirmed MS were prospectively included. One radiologist performed manual segmentations of all high-signal intensity lesions using three 3D FLAIR data sets with different TR of 4800 ms ("$FLAIR_{4800}$"), 8000 ms ("$FLAIR_{8000}$") and 10,000 ms ("$FLAIR_{10,000}$") and two radiologists double-checked it. The main judgment criterion was the overall number of lesions; secondary objectives were the assessment of lesion location, as well as measuring contrast-to-noise ratio (CNR) and signal-to-noise ratio (SNR). A non-parametric Wilcoxon's test was used to compare the differing FLAIR.

Results The $FLAIR_{8000}$ and $FLAIR_{10,000}$ detected significantly more overall lesions per patient as compared with the $FLAIR_{4800}$ [116.1 (±61.7) ($p=0.02$) and 115.8 (±56.3) ($p=0.03$) versus 99.2 (±66.9), respectively]. The $FLAIR_{8000}$ and $FLAIR_{10,000}$ detected four and eight times more cortical or juxta-cortical lesions per patient as compared with $FLAIR_{4800}$ [1.6 (±2.2) ($p=0.001$) and 4.1 (±5.9) ($p=6\times10^{-5}$) versus 0.4 (±1.1), respectively]. CNR was significantly correlated to the TR value. It was significantly higher with $FLAIR_{10,000}$ than it was with $FLAIR_{8000}$ and $FLAIR_{4800}$ [16.3 (±3.5) versus 15 (±2.4) ($p=0.01$) and 12 (±2.2) ($p=2\times10^{-6}$), respectively]

Conclusion An optimized 3D FLAIR with a long TR significantly improved both overall lesion detection and CNR in MS patients as compared to a 3D FLAIR with factory settings.

Keywords Diagnosis · Magnetic resonance imaging · Diagnostic imaging · Multiple sclerosis

Augustin Lecler and C. Bouzad contributed equally to the work and are co-first authors.

Electronic supplementary material The online version of this article (https://doi.org/10.1007/s00415-019-09490-y) contains supplementary material, which is available to authorized users.

✉ Augustin Lecler
alecler@for.paris

[1] Department of Radiology, Fondation Ophtalmologique Adolphe de Rothschild, 25 rue Manin, 75019 Paris, France

[2] Department of Radiology, Bégin Military Teaching Hospital, Saint Mandé, France

[3] Department of Neurology, Fondation Ophtalmologique Adolphe de Rothschild, Paris, France

[4] Clinical Research Unit, Fondation Ophtalmologique Adolphe de Rothschild, Paris, France

Abbreviations

MS	Multiple sclerosis
MRI	Magnetic resonance imaging
FLAIR	Fluid-attenuated inversion recovery
WI	Weighted imaging
CNR	Contrast-to-noise ratio
SNR	Signal-to-noise ratio
TR	Repetition time

Introduction

Multiple sclerosis (MS) is the most frequent chronic inflammatory disease of the central nervous system [1–4]. Magnetic resonance imaging (MRI) has been shown to be the most efficient modality to image MS [5] and has been included in the diagnostic work-up of the disease since 2001 [6, 7]. MRI is also the modality of choice in disease

monitoring and has substantial prognostic value for patients with clinically isolated syndromes suggestive of MS when and if there is conversion to definitive MS [8, 9].

MRI is performed in suspected or confirmed MS as a multisequence protocol including at least one fluid-attenuated inversion recovery (FLAIR) [10, 11], which is the key sequence to detect brain lesions. Three-dimensional (3D) FLAIR is more sensitive than two-dimensional (2D) FLAIR [12–14] when detecting both supra and infra-tentorial lesions [15, 16]. There have been many studies trying to find the best MRI sequence to most accurately detect brain lesions in patients with MS [5, 12–26].

However, there is no consensus concerning acquisition parameters of 3D FLAIR, such as repetition time (TR), echo time (TE) or inversion time (TI), which are the main parameters affecting its contrast and lesion-to-tissue contrast, although they certainly are determining factors in lesions detection.

The aim of our study was to evaluate the diagnostic value of three 3D FLAIR sequences with different TR at 3-Tesla (3T) to detect MS lesions.

Materials and methods

Study design

We conducted a prospective study (NCT 03108573) in a tertiary referral center specializing in neurological diseases. This study was approved by an independent Institutional Research Ethics Board and adhered to the tenants of the Declaration of Helsinki (IRB 2012-A00993-40). Signed informed consent was obtained from all subjects. This study follows the "Standards for Reporting Diagnostic accuracy studies" (STARD) guidelines [27].

27 patients were included. Inclusion criteria were: (a) age over 18 years; (b) confirmed diagnosis of MS as defined by the 2017 McDonald criteria [7]. Patients with any MRI contraindication were not included. Exclusion criteria were (a) insufficient quality of MRI for interpretation; (b) absence of at least one 3D FLAIR sequence tested. Selection of patients is shown in Supplementary Fig. 1.

MRI protocol

All MRIs were performed on the same 3T Philips Ingenia device (Philips Medical System) with a 16-channel head coil. Each patient underwent the usual recommended protocol [11] used in our unit for MS follow-up, including a 3D T1 Turbo Spin Echo (TSE) (TR: 350 ms, TE: 28 ms, slice thickness: 1 mm, matrix: 256 × 203 mm, FOV: 230 × 230 mm), an axial high-resolution TSE T2-weighted sequence (TR: 4545 ms, TE: 80 ms, slice thickness: 3 mm, matrix: 384 × 299 mm, FOV: 230 × 230 mm) and a 3D FLAIR with factory settings with a TR of 4800 ms labelled as "$FLAIR_{4800}$" corresponding to the 3D FLAIR with factory settings provided by the vendor. This protocol was completed by two other 3D FLAIR sequences chosen among eight 3D FLAIR with different TR (varying from 4800 to 13,000 ms) tested on three MS patients not included in our study, as planned in the study design. These two selected 3D FLAIR provided the best subjective contrast between the

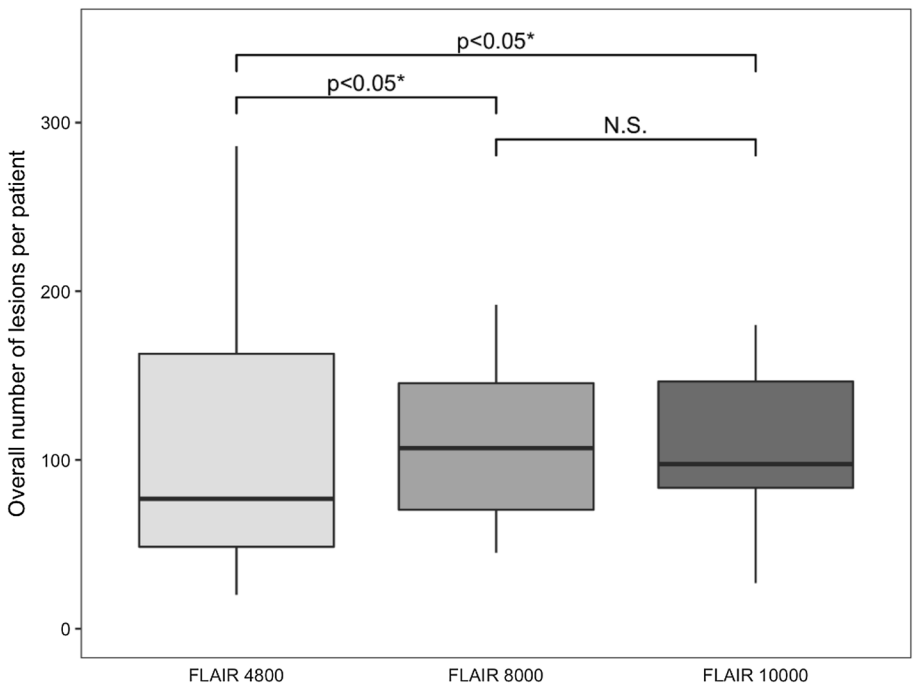

Fig. 1 Boxplots showing the overall number of FLAIR high-signal intensity lesions per patient according to each 3D FLAIR. *Significant differences after appropriate statistical correction. Median is represented by the horizontal black line and interquartile range by the upper and lower limits of the box. *FLAIR* fluid-attenuated inversion recovery, *N.S.* non-significant

brain lesions and the normal-appearing white matter and the best contrast-to-noise ratio (CNR). The first one had a TR of 8000 ms, labelled as "$FLAIR_{8000}$", and the second one a TR of 10,000 ms, labelled as "$FLAIR_{10,000}$". All three 3D FLAIR sequences were performed at the end of the imaging protocol and their order was randomized between participants to overcome a possible effect of contrast administration on lesion detection. The TI value was modified to allow for a satisfying fluid suppression, defined by a cerebro-spinal fluid signal close to 0. The turbo factor was chosen to be increased in both sequences with high TR to partially compensate for the increased acquisition time induced by higher TR and to maintain clinically acceptable examination duration. The effective TE was set to automatically be as short as possible. All of the other acquisition parameters remained constant and are detailed in Table 1. All 3D FLAIR sequences were acquired with a "3D Brainview" mode using optimized variable refocusing flip angles.

An intravenous contrast injection of a single dose of Gadobutrol (Bayer HealthCare) was performed for all patients at least 5 minutes before the MRI acquisition, as recommended [11].

Image and data analysis

MS lesions segmentation and feature extraction

All 81 3D FLAIR acquisitions (three for each patient) were transferred and anonymized on a dedicated research reading workstation using OsiriX imaging software (Pixmeo) and processed with an in-house Matlab image segmentation and statistics toolkit. All FLAIR high-signal intensity lesions were segmented manually in the axial plane during a dedicated reading session by one junior radiologist (C.B) blinded to clinical data. Each 3D FLAIR data set segmentation lasted approximately 3 h. Segmentations were corrected during a second consensus reading session by two senior neuroradiologists (A.L and J.S) with 8 and 20 years of experience, respectively, blinded to clinical data and sequence identity. There were no subjective differences in image contrast between the three different 3D FLAIRs evaluated, thus readers were effectively blinded. They added missing lesions, deleted high-signal areas that were not MS lesions and redefined the contours of the segmented lesions. Only lesions measuring at least 2 mm^3 were considered. Each lesion was labeled according to their location, based on the McDonald criteria: infra-tentorial, periventricular white matter, deep white matter, cortical/juxta-cortical [7]. All segmentations occurred in a random order so that the readers did not process sequences from the same patient or with the same TR

Table 1 Acquisition and reconstruction parameters for the 3D FLAIR sequences

Parameters	3D $FLAIR_{4800}$	3D $FLAIR_{8000}$	3D $FLAIR_{10,000}$
TR (ms)	4800	8000	10,000
Effective TE (ms) (mean) [min–max]	253 [244–271]	339 [326–364]	394 [335–425]
TI (ms)	1650	2400	2600
FOV (mm × mm)	240×240	240×240	240×240
Acquisition matrix size (mm × mm)	240×240	240×240	240×240
Reconstructed matrix size (mm × mm)	256×256	256×256	256×256
Acquisition plane	Sagittal	Sagittal	Sagittal
Slice thickness (mm)	1	1	1
Gap (mm)	0	0	0
Actual voxel size (mm)	1×1x1	1×1x1	1×1x1
Reconstructed voxel size (mm)	0.94×0.94x0.5	0.94×0.94x0.5	0.94×0.94x0.5
Number of slices	365	365	365
Scan time duration (ms)	3 min 36 s	4 min 24 s	4 min 40 s
Turbo factor	130	180	215
Bandwidth (Hz)	947	947	947
Flip angle (°)	40	40	40
NEX	1	1	1
Acceleration factor (SENSE P×S)	3×2	3×2	3×2
Fat suppression	SPIR	SPIR	SPIR

TR repetition time, *TE* echo-time, *TI* inversion time, *FOV* field of view, *FLAIR* fluid-attenuated inversion recovery, *NEX* number of excitations, *SPIR* spectral presaturation with inversion recovery, *SENSE* SENSitivity encoding

in a row. Once the segmentation and labelling were done, the toolkit provided each patient and each FLAIR sequence a table with a list of all individual segmented lesions and their features (location label, signal intensity, and compacity). Two segmented areas were considered separate lesions if they had no neighbour segmented high-intensity voxel, meaning that a confluent lesion was considered a single high-volume lesion. Finally, for each FLAIR sequence and each patient, the total number of lesions and the number of lesions for each location was available. The pre-specified primary outcome measure was the total number of lesions. Secondary outcome measures were the number of lesions for each location.

Signal and contrast properties

To measure the signal-to-noise ratio (SNR) of the FLAIR sequences, we used the NEMA (National Electrical Manufacturers Association) method [28] that needs two images acquired within 5 min of each other with the exact same imaging parameters in five patients. Those two images were then subtracted to produce a third one. On each subtracted sequence for each patient, we placed two regions of interest (ROI) in normal-appearing white matter of the right and left centrum semi-ovale to measure their signal intensity (SI) and to obtain the mean white matter SI (SI_{WM}). We took the standard deviation (SD) of the value of the ROIs and extracted the average SD of the noise. For the CNR of the lesions, we manually placed an ROI in each sequence for each patient in two non-enhancing lesions of significant size to measure their SI and obtain the mean lesion SI (SI_{lesion}). Those lesions had to be visible on all sequences and were the same on each sequence. Then, we calculated the SNR using the formula:$\mathrm{SNR} = \frac{SI_{WM} \times \sqrt{2}}{SD}$ and the CNR as following: $\mathrm{CNR} = \frac{SI_{lesion} - SI_{WM}}{SD}$.

Statistical analysis

Analyses were conducted by a statistical analyst (H.P) with 10 years of experience, using the R software version 3.3.2 [29]. Categorical and continuous data were reported as a number (%) as appropriate. Continuous data were reported as median with interquartile ranges or mean values ± standard deviation as appropriate. The non-parametric Wilcoxon's test was used to compare the different 3D FLAIR, using the Streitberg–Rohmel algorithm in case of a tie. Spearman correlation coefficients were calculated to determine the correlation between the number of lesions and EDSS scores. *p* values below 0.05 were considered significant. Since multiple tests were performed, Bonferroni adjustment was used with an α level adjusted to a significance level of 0.005. The sample size was calculated based on a minimum expected mean difference of 10% in detecting MS lesions and 5% in CNR between the optimized FLAIR sequences and the FLAIR sequence with factory settings and a common standard deviation of 0.15. These values were obtained from three MS patients not included in our study. The statistical power was set at 0.9 and the significance criterion was set to 0.05, with a two-tailed analysis [30]. Twenty-one patients would be necessary for this statistical analysis. A final objective of 27 patients was set to anticipate secondary exclusions and non-exploitable data.

Results

Patient characteristics

Twenty-seven patients with a confirmed diagnosis of MS [14 males and 13 females, mean age 37 years old ± 10.7 (SD)] were included. Mean EDSS score was 3.2 ± 2.1 (SD). The mean disease duration was 13.6 years ± 9.2 (SD). The MS phenotype composition was as follows: 21 (78%) relapsing remittent, 4 (15%) secondary progressive and 2 (7%) primary progressive.

Number of FLAIR high-signal intensity lesions

Over the 27 patients, a total of 8941 lesions were segmented.

$FLAIR_{8000}$ and $FLAIR_{10,000}$ detected significantly more overall lesions per patient as compared with the $FLAIR_{4800}$ [mean 116.1 (±61.7) ($p = 0.02$) and 115.8 (±56.3) ($p = 0.03$) versus 99.2 (±66.9), respectively] (Fig. 1).

$FLAIR_{8000}$ and $FLAIR_{10,000}$ detected four and eight times more cortical or juxta-cortical lesions per patient as compared with $FLAIR_{4800}$ [mean 1.6 (±2.2) ($p = 0.001$) and 4.1 (±5.9) ($p = 6.10^{-5}$) versus 0.4 (±1.1), respectively] (Fig. 2 and Supplementary Fig. 2).

$FLAIR_{8000}$ detected significantly more periventricular and deep white matter lesions than $FLAIR_{4800}$ [mean 76.3 (±50.2) versus 64 (±40.7) ($p = 0.009$) and 21.6 (±18.7) versus 20.6 (±31) ($p = 0.04$), respectively]. $FLAIR_{10,000}$ detected significantly more periventricular white matter lesions than $FLAIR_{4800}$ [mean 72.3 (±50) versus 64 (±40.7) ($p = 0.02$)] (Supplementary Fig. 2).

There was no significant difference between $FLAIR_{8000}$ and $FLAIR_{10,000}$ regardless of location. Table 2 provides detailed data on lesions per sequence and location.

Four (15%) patients had at least one cortical or juxta-cortical lesion visible on $FLAIR_{8000}$ or $FLAIR_{10,000}$ and none on $FLAIR_{4800}$. Three (11%) patients had at least one infra-tentorial lesion visible on $FLAIR_{8000}$ or $FLAIR_{10,000}$ and none on $FLAIR_{4800}$, respectively.

There was no significantly higher correlation between EDSS scores and the number of lesions on $FLAIR_{8000}$ or $FLAIR_{10,000}$ as compared to the $FLAIR_{4800}$.

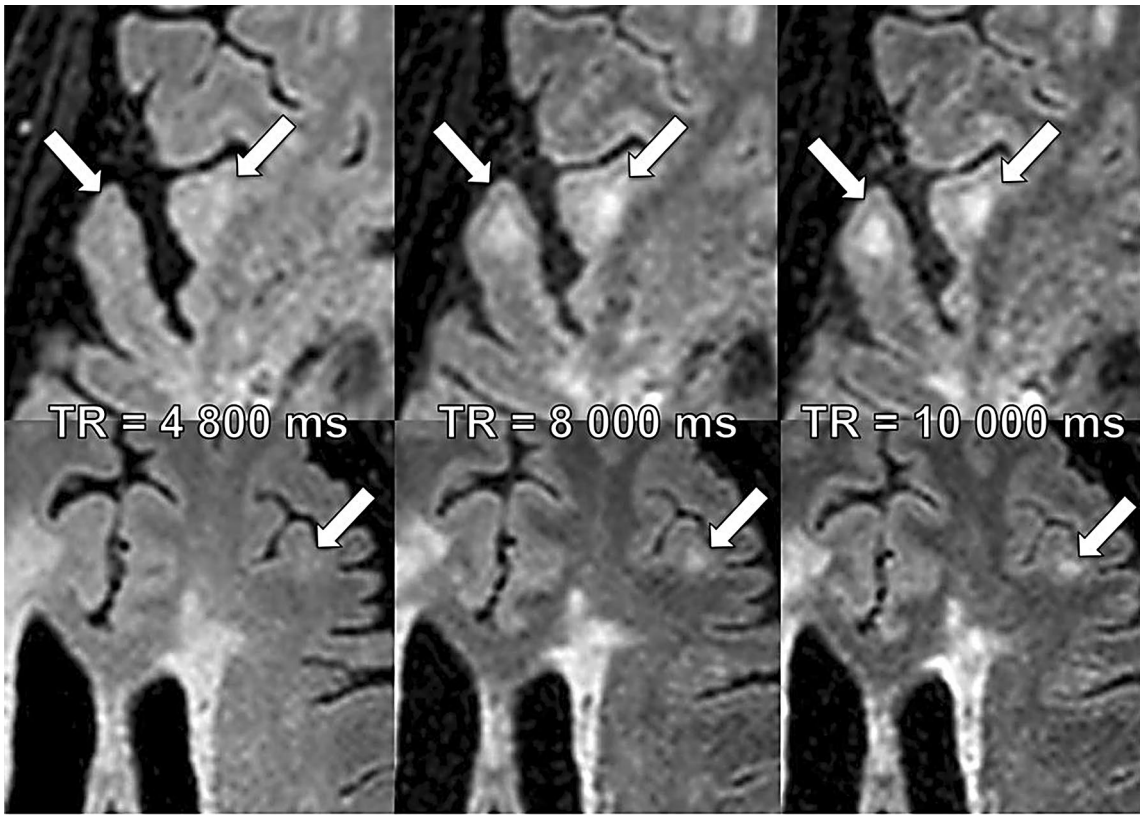

Fig. 2 Examples of juxta-cortical lesions (white arrows) hardly visible on the $FLAIR_{4800}$ and easily detected on the $FLAIR_{8000}$ and $FLAIR_{10,000}$ sequences. *FLAIR* fluid-attenuated inversion recovery

Table 2 Total number of segmented lesions per patient and location according to the three different 3D FLAIR

	Number of lesions			Relative comparison[§]		
	$FLAIR_{4800}$	$FLAIR_{8000}$	$FLAIR_{10,000}$	4800 VS 8000	4800 VS 10,000	8000 VS 10,000
Patients	27	27	27			
Overall	2678	3136	3127			
Mean (SD)	99.2 (66.9)	116.1 (61.7)	115.8 56.3)	$p=0.02$*	$p=0.03$*	$p=0.7$
Infra-tentorial	382	448	544			
Mean (SD)	14.2 (10.6)	16.6 (13.1)	20.2 (15.4)	$p=0.2$	$p=0.1$	$p=0.6$
Cortical or juxta-cortical	12	44	111			
Mean (SD)	0.4 (1.1)	1.6 (2.2)	4.1 (5.9)	$p=0.001$*	$p=6\times10^{-5}$*	$p=0.08$
Periventricular	1729	2061	1951			
Mean (SD)	64.0 (40.7)	76.3 (50.2)	72.3 (50.3)	$p=0.04$*	$p=0.5$	$p=0.2$
Deep white matter	555	583	521			
Mean (SD)	20.6 (31.1)	21.6 (18.6)	19.3 (15.9)	$p=0.009$*	$p=0.02$*	$p=0.4$

FLAIR fluid-attenuated inversion recovery, *SD* standard deviation

*Significant differences after appropriate statistical correction

[§]*p* value after comparison of the two groups with the non-parametric Wilcoxon's test

Signal-to-noise and contrast-to-noise ratios

CNR was significantly correlated to the TR value. It was significantly higher with $FLAIR_{10,000}$ as compared to $FLAIR_{8000}$ and $FLAIR_{4800}$ [16.3 (±3.5) versus 15 (±2.4) ($p=0.01$) and 12 (±2.2) ($p=2\times10^{-6}$), respectively] (Fig. 3).

SNR was inversely proportional to the TR value. It was significantly higher with $FLAIR_{4800}$ as compared to $FLAIR_{8000}$ and $FLAIR_{10,000}$ [36.6 (±4) versus 29.7(±3.5) ($p=1\times10^{-8}$) and 27.7 (±4.5) ($p=1\times10^{-7}$), respectively] (Fig. 3). Table 3 provides detailed data on SNR and CNR. Figure 4 shows the noise pictures calculated for each 3D FLAIR.

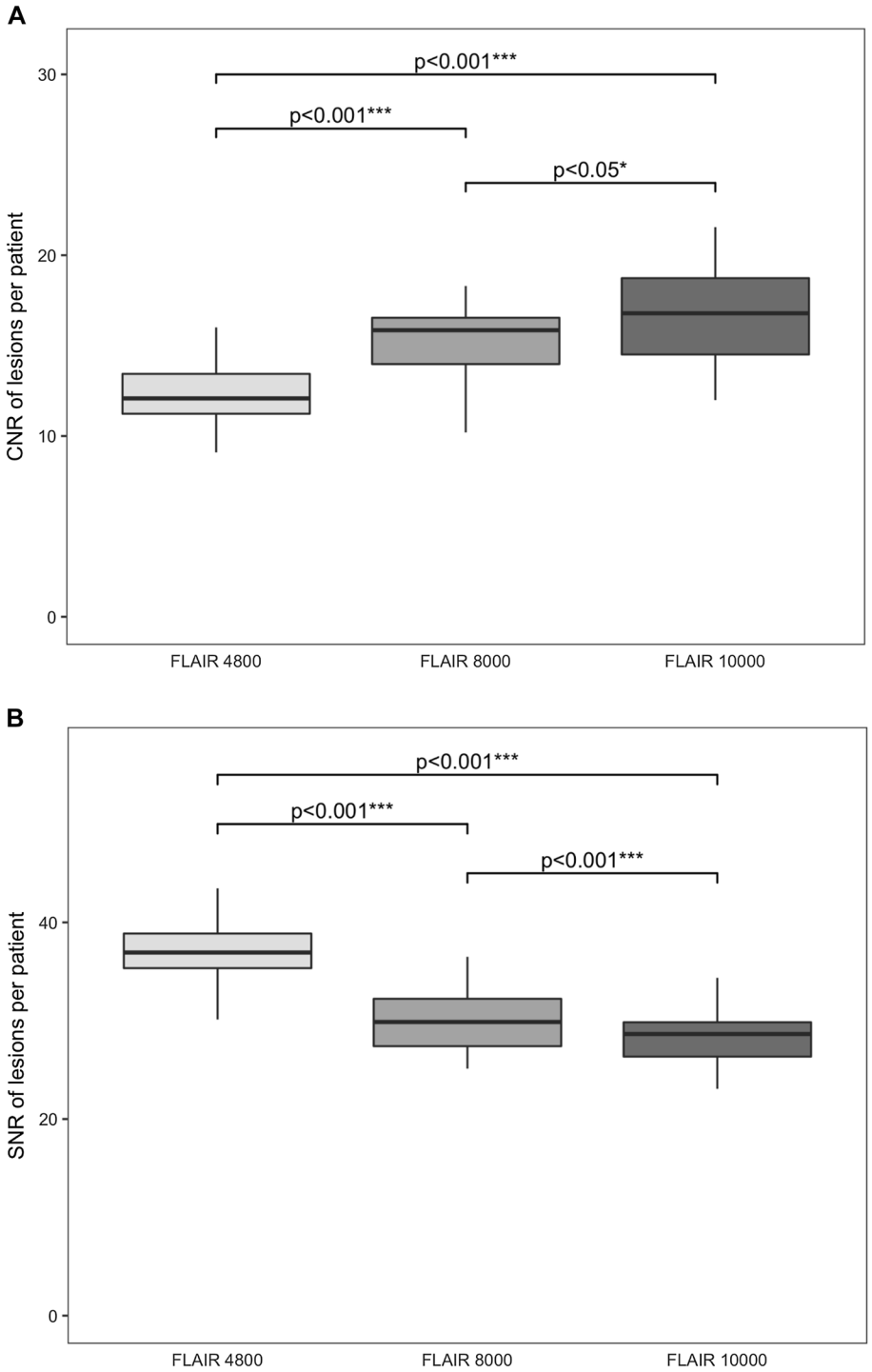

Fig. 3 Boxplots showing CNR (**a**) and SNR (**b**) of FLAIR High-intensity lesions per patient. *Significant differences after appropriate statistical correction. Median is represented by the horizontal black line and interquartile range by the upper and lower limits of the box. *FLAIR* fluid-attenuated inversion recovery, *CNR* contrast-to-noise ratio, *SNR* signal-to-noise ratio

Table 3 Mean values of SNR and CNR and pair-wise comparison of those values

	Values			Relative comparison[§]			
	$FLAIR_{4800}$	$FLAIR_{8000}$	$FLAIR_{10,000}$	4800 VS 8000		4800 VS 10,000	8000 VS 10,000
Patients	27	27	27				
SNR (SD)	36.6 (4)	29.7 (3.5)	27.7 (4.5)	$p = 1 \times 10^{-8}$*	$p = 1 \times 10^{-7}$*		$p = 0.001$*
CNR (SD)	12.0 (2.2)	15.0 (2.4)	16.3 (3.5)	$p = 5 \times 10^{-7}$*	$p = 2 \times 10^{-6}$*		$p = 0.01$*

SNR signal-to-noise ratio, *CNR* contrast-to-noise ratio, *FLAIR* fluid-attenuated inversion recovery, *SD* standard deviation

*Significant differences after appropriate statistical correction

[§]*p* value after comparison of the two groups with the non-parametric Wilcoxon's test

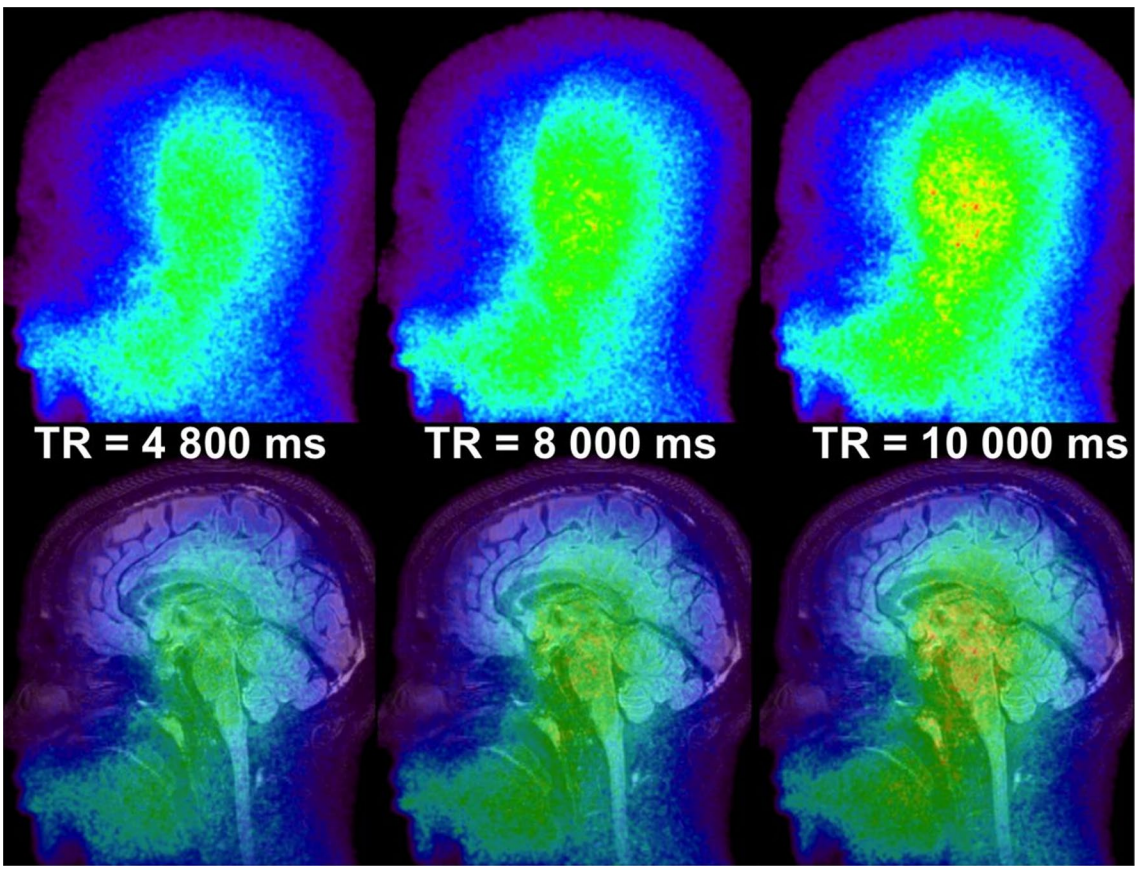

Fig. 4 Noise pictures (acquisition without radiofrequency or gradient emission) on the three 3D FLAIR sequences; warm colors representing high noise values. On the upper line: 5 mm Maximum Intensity Projection (MIP) representation of the noise; on the lower line: combination of the noise and the FLAIR images. The higher the TR, the higher is the noise. Note that noise increases from outside to inside. *FLAIR* fluid-attenuated inversion recovery, *TR* repetition time

Discussion

Our study showed that an optimized 3D FLAIR sequence with a long TR of 8000 or 10,000 ms significantly improved both overall lesion detection and CNR in MS patients as compared to a 3D FLAIR with factory settings with a TR of 4800 ms.

There have been many studies trying to find the best MRI sequence to most accurately detect brain lesions in patients with MS, such as T2-WI [5], proton-density-WI [12], 2D FLAIR [13, 16, 17], magnetization transfer [18], magnetization-prepared rapid acquisition with gradient echo (MPRAGE) [19], 3D FLAIR [12, 14–16, 20], double inversion recovery (DIR) [16, 21–23] or phase-sensitive inversion

recovery sequence (PSIR) [24, 25]. There also have been studies trying to improve the detection rate by combining sequences, such as the PT2 [31] or the FLAIR^2 [32], or by subtraction [33]. However, we found only one study that specifically dealt with 3T 3D FLAIR sequence optimization for identifying MS lesions by modifying the TE. In this study, the authors developed a "3D FLAIRED" (FLAIR Enhanced Detection) with an iterative approach based on theoretical considerations. They obtained and analyzed a 3D spin-echo FLAIR with a longer contrast-equivalent TE than the effective TE of a 3D FLAIR (600 ms versus 450 ms) without modifying the TR values, kept constant at 7000 ms. They showed that lesion recognition was improved in both supratentorial and infra-tentorial regions and that detection of cortical lesions increased with the 3D FLAIRED [20].

The better performance of our FLAIR$_{8000}$ and FLAIR$_{10,000}$ sequence over the FLAIR$_{4800}$ may be explained by a better contrast existing between the lesion and its environment, which is obtained by increasing the TR. The main parameters affecting the contrast of the FLAIR are the TR, the TE, the TI and the flip angles. The TR seems to be a relevant parameter to study since it is the main determinant of the intensity of the T2 signal. It is related to the T2 effect and the augmentation of the effective TE attenuates the normal white matter signal, making lesions more easily depictable [20, 34]. We subjectively chose two TR of 8000 and 10,000 ms for our optimized 3D FLAIR sequences because they provided the best subjective contrast between MS lesions and the normal-appearing white matter while preserving a reasonable acquisition time with a constant resolution. Interestingly, these values are very close to the TR of 7000 ms of the optimized FLAIRED sequence, which was considered the most sensitive in the detection of MS lesions [20], and are the same as those proposed to reach near optimum contrast and high multisection efficiency in a previous 2D FLAIR optimization study at 1.5 T [34].

A longer TR significantly increased the CNR in our series, allowing higher confidence in discriminating brain lesions from normal-appearing white matter. However, we did not find any statistically significant difference between the number of lesions depicted on the FLAIR$_{8000}$ and FLAIR$_{10,000}$, which might be partially explained by a decreased SNR on FLAIR$_{10,000}$. Our results pointed out an inverse correlation between SNR and TR that seemed paradoxical since SNR normally increases with TR. The two other parameters that were different between sequences (the effective TE and the turbo factor) explain the decrease of SNR: the higher the TR, the higher both the effective TE and the turbo factor were set. The SNR has an inverse correlation with those two parameters.

We chose to compare FLAIR$_{8000}$ and FLAIR$_{10,000}$ to the 3D FLAIR$_{4800}$ with factory settings provided by most constructors at the time of the beginning of the study. It is important to point out that the factory settings of the 3D FLAIR proposed by most vendors are tested and developed on healthy volunteers and are not optimized to depict pathological abnormalities of signal even though they offer a good cerebro-spinal fluid suppression and a good SNR. We showed that this 3D FLAIR$_{4800}$ with factory settings depicted significantly fewer lesions and therefore should be modified and optimized before using it for clinical practice.

Both CMSC [11] and MAGNIMS [10] groups recommend to perform a FLAIR as a key sequence in MS patients. They provide suggestions on minimal technical specifications such as the maximum slice thickness, the spatial resolution, the voxel size and the duration time of the protocol. We believe that guidelines should also include recommendations on key parameters such as the TR. A TR of 8000 ms seems to be a good compromise for the FLAIR sequence, with a reasonable acquisition time (4.5 min in our study) and good SNR and CNR, meaning an easier and more comfortable reading. The 3D FLAIR is widely available in all centers, and the modification of its parameters might be easily feasible on most clinical scanners. It is simple, and it may facilitate standardization of protocols among different centers worldwide. It requires no post-processing time nor any specific software, as compared with other efficient sensitive sequences such as the FLAIR^2 or the PT2 [31, 32]. It is more accessible in clinical practice than other very effective sequences in depicting MS lesions, such as the DIR or the PSIR. Those sequences are known to be very effective in depicting cortical lesions, especially when combined. The very good spatial resolution of the PSIR was reported to help by compensating for the mediocrity of delineation and classification of cortical lesions on the DIR sequence [24]. Yet, a recent study [35] showed that, at 3 T, a 3D FLAIR sequence presented with a better SNR than a DIR sequence with a similar contrast quality and an inferior time of acquisition, suggesting that the 3D FLAIR was the best sequence to identify cortical lesions. For these reasons, we now routinely perform a FLAIR$_{8000}$ for suspected MS and follow-up in our institution.

An increase of the performance of detecting MS lesions presents two major direct advantages for the patients: an earlier diagnosis and prognosis classification (especially for clinically or radiologically isolated syndromes) [36, 37] and better follow-up thanks to an earlier diagnosis of new lesions. Those two elements have a deep impact on both the therapeutic decision-making and the patient's treatment [38, 39]. We found that 4 (15%) and 3 (11%) patients had at least one cortical or juxta-cortical lesion or one infratentorial lesion, respectively, on FLAIR$_{8000}$ or FLAIR$_{10,000}$ and none with a 3D FLAIR$_{4800}$ with factory settings. This is clinically relevant since these two locations are among the four main locations taken into account for diagnosing MS [7]. Moreover, we found significantly more cortical or

juxta-cortical and peri-ventricular lesions using $FLAIR_{8000}$ and $FLAIR_{10,000}$ as compared with a 3D $FLAIR_{4800}$ with factory settings. This better performance has a valuable clinical impact since several studies showed that those lesions were better correlated to disability, cognitive decline and even to progression of the disease as compared to effects from periventricular and deep white matter lesions [20, 40, 41]. Those lesions exist at the onset of the disease, even in patients with radiologically isolated syndromes [42].

Our study has some limitations: first, the results of this prospective study are somewhat limited by the relatively small number of patients and by the fact that the data are from one machine, thus it is impossible to fully determine their generalizability. Multicenter studies, including a larger sample size, are necessary to confirm the results and to validate them across various MRI manufacturers. Second, we did not perform a direct comparison with other sequences such as DIR or PSIR or other advanced techniques such as PT2, FLAIRED or $FLAIR^2$, but our study was not designed for this since its aim was to evaluate the impact of different TR on the FLAIR sequence. We also did not perform a comparison with T2-weighted scans, although using optimized FLAIR sequences might be interesting for detecting infratentorial lesions. Third, we did not study the impact of other parameters on detecting MS lesions although the optimization of all parameters could further increase the accuracy of the FLAIR sequence and should be evaluated in further studies. Fourth, although this study aimed to compare FLAIR sequences by modifying their TR lengths, other important parameters (TE, TI, turbo factor) have also been accordingly modified, meaning that changing the TR alone without further adjustments would not necessarily result in optimized lesion results. TE was not kept identical across the three different FLAIR sequences, but was set to the minimum possible value for all sequences to maximize the signal-to-noise ratio, which might have modified the contrast. However, its increase across the three different FLAIR sequences was an effect of both the increase of the TR and the turbo spin factor and was directly proportional to the increase of the TR. Therefore, TE is substantially less likely to be a determinant of the improved contrast of optimized FLAIR sequences in our study, as compared to the TR, which is considered the most important determinant of the FLAIR signal by minimizing the T1 component and increasing the T2 component. Therefore, we can consider that TR was the main parameter which substantially modified the contrast across the three FLAIR sequences, thus explaining the improved detection of MS lesions.

In conclusion, our study showed that an optimized 3D FLAIR sequence with a long TR of 8000 or 10,000 ms significantly improved both overall lesion detection and CNR in MS patients as compared to the widely used factory-settings 3D FLAIR with a TR of 4800. It advocates for going beyond the standardization of protocols and standardize sequences themselves to improve results' reproducibility and therefore patients' care.

Acknowledgements Laura McMaster provided professional English-language medical editing of this article.

Compliance with ethical standards

Conflicts of interest No conflicting relationship exists for any author.

Ethical approval This study has been approved by an institutional research ethics board.

References

1. Geurts JJG, Calabrese M, Fisher E, Rudick RA (2012) Measurement and clinical effect of grey matter pathology in multiple sclerosis. Lancet Neurol 11:1082–1092. https://doi.org/10.1016/S1474-4422(12)70230-2
2. Klaver R, De Vries HE, Schenk GJ, Geurts JJG (2013) Grey matter damage in multiple sclerosis: a pathology perspective. Prion 7:66–75. https://doi.org/10.4161/pri.23499
3. Messina S, Patti F (2014) Gray matters in multiple sclerosis: cognitive impairment and structural MRI. Mult Scler Int 2014:609694. https://doi.org/10.1155/2014/609694
4. Pirko I, Lucchinetti CF, Sriram S, Bakshi R (2007) Gray matter involvement in multiple sclerosis. Neurology 68:634–642. https://doi.org/10.1212/01.wnl.0000250267.85698.7a
5. Runge VM, Price AC, Kirshner HS et al (1984) Magnetic resonance imaging of multiple sclerosis: a study of pulse-technique efficacy. AJR Am J Roentgenol 143:1015–1026. https://doi.org/10.2214/ajr.143.5.1015
6. McDonald WI, Compston A, Edan G et al (2001) Recommended diagnostic criteria for multiple sclerosis: guidelines from the international panel on the diagnosis of multiple sclerosis. Ann Neurol 50:121–127
7. Thompson AJ, Banwell BL, Barkhof F et al (2017) Diagnosis of multiple sclerosis: 2017 revisions of the McDonald criteria. Lancet Neurol. https://doi.org/10.1016/S1474-4422(17)30470-2
8. Barkhof F, Filippi M, Miller DH et al (1997) Comparison of MRI criteria at first presentation to predict conversion to clinically definite multiple sclerosis. Brain J Neurol 120(Pt 11):2059–2069
9. Tintoré M, Rovira A, Martínez MJ et al (2000) Isolated demyelinating syndromes: comparison of different MR imaging criteria to predict conversion to clinically definite multiple sclerosis. AJNR Am J Neuroradiol 21:702–706
10. Rovira À, Wattjes MP, Tintoré M et al (2015) Evidence-based guidelines: MAGNIMS consensus guidelines on the use of MRI in multiple sclerosis-clinical implementation in the diagnostic process. Nat Rev Neurol 11:471–482. https://doi.org/10.1038/nrneurol.2015.106
11. Traboulsee A, Simon JH, Stone L et al (2016) Revised recommendations of the consortium of MS centers task force for a standardized MRI protocol and clinical guidelines for the diagnosis and follow-up of multiple sclerosis. AJNR Am J Neuroradiol 37:394–401. https://doi.org/10.3174/ajnr.A4539
12. Gramsch C, Nensa F, Kastrup O et al (2015) Diagnostic value of 3D fluid attenuated inversion recovery sequence in multiple sclerosis. Acta Radiol Stockh Swed 1987 56:622–627. https://doi.org/10.1177/0284185114534413

13. Okuda T, Korogi Y, Shigematsu Y et al (1999) Brain lesions: when should fluid-attenuated inversion-recovery sequences be used in MR evaluation? Radiology 212:793–798. https://doi.org/10.1148/radiology.212.3.r99se07793
14. Tan IL, van Schijndel RA, Pouwels PJW et al (2002) Serial isotropic three-dimensional fast FLAIR imaging: using image registration and subtraction to reveal active multiple sclerosis lesions. AJR Am J Roentgenol 179:777–782. https://doi.org/10.2214/ajr.179.3.1790777
15. Bink A, Schmitt M, Gaa J et al (2006) Detection of lesions in multiple sclerosis by 2D FLAIR and single-slab 3D FLAIR sequences at 3.0 T: initial results. Eur Radiol 16:1104–1110. https://doi.org/10.1007/s00330-005-0107-z
16. Moraal B, Roosendaal SD, Pouwels PJW et al (2008) Multi-contrast, isotropic, single-slab 3D MR imaging in multiple sclerosis. Eur Radiol 18:2311–2320. https://doi.org/10.1007/s00330-008-1009-7
17. Hashemi RH, Bradley WG, Chen DY et al (1995) Suspected multiple sclerosis: MR imaging with a thin-section fast FLAIR pulse sequence. Radiology 196:505–510. https://doi.org/10.1148/radiology.196.2.7617868
18. Iannucci G, Rovaris M, Giacomotti L et al (2001) Correlation of multiple sclerosis measures derived from T2-weighted, T1-weighted, magnetization transfer, and diffusion tensor MR imaging. AJNR Am J Neuroradiol 22:1462–1467
19. Nelson F, Poonawalla A, Hou P et al (2008) 3D MPRAGE improves classification of cortical lesions in multiple sclerosis. Mult Scler Houndmills Basingstoke Engl 14:1214–1219. https://doi.org/10.1177/1352458508094644
20. Polak P, Magnano C, Zivadinov R, Poloni G (2012) 3D FLAIRED: 3D fluid attenuated inversion recovery for enhanced detection of lesions in multiple sclerosis. Magn Reson Med 68:874–881. https://doi.org/10.1002/mrm.23289
21. Geurts JJG, Pouwels PJW, Uitdehaag BMJ et al (2005) Intracortical lesions in multiple sclerosis: improved detection with 3D double inversion-recovery MR imaging. Radiology 236:254–260. https://doi.org/10.1148/radiol.2361040450
22. Vural G, Keklikoğlu HD, Temel Ş et al (2013) Comparison of double inversion recovery and conventional magnetic resonance brain imaging in patients with multiple sclerosis and relations with disease disability. Neuroradiol J 26:133–142. https://doi.org/10.1177/197140091302600201
23. Wattjes MP, Lutterbey GG, Gieseke J et al (2007) Double inversion recovery brain imaging at 3T: diagnostic value in the detection of multiple sclerosis lesions. AJNR Am J Neuroradiol 28:54–59
24. Favaretto A, Poggiali D, Lazzarotto A et al (2015) The parallel analysis of phase sensitive inversion recovery (PSIR) and double inversion recovery (DIR) images significantly improves the detection of cortical lesions in multiple sclerosis (MS) since clinical onset. PLoS ONE 10:e0127805. https://doi.org/10.1371/journal.pone.0127805
25. Nelson F, Poonawalla AH, Hou P et al (2007) Improved identification of intracortical lesions in multiple sclerosis with phase-sensitive inversion recovery in combination with fast double inversion recovery MR imaging. AJNR Am J Neuroradiol 28:1645–1649. https://doi.org/10.3174/ajnr.A0645
26. Lecler A, El Sanharawi I, El Methni J et al (2019) Improving detection of multiple sclerosis lesions in the posterior fossa using an optimized 3D-FLAIR sequence at 3T. AJNR Am J Neuroradiol. https://doi.org/10.3174/ajnr.A6107
27. Bossuyt PM, Reitsma JB, Bruns DE et al (2015) STARD 2015: an updated list of essential items for reporting diagnostic accuracy studies. Radiology 277:826–832. https://doi.org/10.1148/radiol.2015151516
28. Goerner FL, Clarke GD (2011) Measuring signal-to-noise ratio in partially parallel imaging MRI. Med Phys 38:5049–5057. https://doi.org/10.1118/1.3618730
29. R Core Team (2019) R: a language and environment for statistical computing. R Foundation for Statistical Computing, Vienna, Austria, 2019. https://www.R-project.org Accessed 11 Mar 2019
30. Eng J (2003) Sample size estimation: how many individuals should be studied? Radiology 227:309–313. https://doi.org/10.1148/radiol.2272012051
31. Gaitán MI, Yañes P, Sati P et al (2016) Optimal detection of infratentorial lesions with a combined dual-echo MRI sequence: "PT2". Mult Scler Houndmills Basingstoke Engl 22:1367–1370. https://doi.org/10.1177/1352458515615226
32. Wiggermann V, Hernández-Torres E, Traboulsee A et al (2016) FLAIR2: a combination of FLAIR and T2 for improved MS lesion detection. AJNR Am J Neuroradiol 37:259–265. https://doi.org/10.3174/ajnr.A4514
33. Moraal B, Wattjes MP, Geurts JJG et al (2010) Improved detection of active multiple sclerosis lesions: 3D subtraction imaging. Radiology 255:154–163. https://doi.org/10.1148/radiol.09090814
34. Rydberg JN, Riederer SJ, Rydberg CH, Jack CR (1995) Contrast optimization of fluid-attenuated inversion recovery (FLAIR) imaging. Magn Reson Med 34:868–877
35. Kolber P, Montag S, Fleischer V et al (2015) Identification of cortical lesions using DIR and FLAIR in early stages of multiple sclerosis. J Neurol 262:1473–1482. https://doi.org/10.1007/s00415-015-7724-5
36. Filippi M, Rocca MA, Ciccarelli O et al (2016) MRI criteria for the diagnosis of multiple sclerosis: MAGNIMS consensus guidelines. Lancet Neurol 15:292–303. https://doi.org/10.1016/S1474-4422(15)00393-2
37. Wattjes MP, Harzheim M, Kuhl CK et al (2006) Does high-field MR imaging have an influence on the classification of patients with clinically isolated syndromes according to current diagnostic mr imaging criteria for multiple sclerosis? AJNR Am J Neuroradiol 27:1794–1798
38. Tur C, Thompson AJ (2015) Early accurate diagnosis crucial in multiple sclerosis. Practitioner 259(21–27):2–3
39. Noyes K, Weinstock-Guttman B (2013) Impact of diagnosis and early treatment on the course of multiple sclerosis. Am J Manag Care 19:s321–331
40. van Munster CEP, Jonkman LE, Weinstein HC et al (2015) Gray matter damage in multiple sclerosis: impact on clinical symptoms. Neuroscience 303:446–461. https://doi.org/10.1016/j.neuroscience.2015.07.006
41. Harrison DM, Roy S, Oh J et al (2015) Association of cortical lesion burden on 7-T magnetic resonance imaging with cognition and disability in multiple sclerosis. JAMA Neurol 72:1004–1012. https://doi.org/10.1001/jamaneurol.2015.1241
42. Mike A, Glanz BI, Hildenbrand P et al (2011) Identification and clinical impact of multiple sclerosis cortical lesions as assessed by routine 3T MR imaging. AJNR Am J Neuroradiol 32:515–521. https://doi.org/10.3174/ajnr.A2340